

Electronic Supporting Information

Thick and Freestanding MXene/PANI Pseudocapacitive Electrodes with Ultra-high Specific Capacitance

Armin Vahid Mohammadi¹, Jorge Moncada², Hengze Chen¹, Emre Kayali¹, Jafar Orangi¹,
Carlos A. Carrero², Majid Beidaghi^{1,*}

¹ Department of Mechanical and Materials Engineering, Auburn University, Auburn, AL 36849,
USA

² Department of Chemical Engineering, Auburn University, Auburn, AL 36849, USA

* Corresponding author: mbeidaghi@auburn.edu

Characterization of hybrid Ti₃C₂T_x/PANI electrodes with different PANI contents

In order to understand the effect of the amount of deposited PANI on the performance of electrodes, hybrid Ti₃C₂T_x/PANI flakes were prepared using different Ti₃C₂T_x to aniline ratios in the synthesis process. **Fig. S1** shows the XRD patterns of the films prepared using MXene to aniline weight ratios of 1:2, 1:4, and 1:500. As the ratio of aniline increases, the (0002) peak of MXene in the fabricated freestanding film shifts to lower angles which is an indication of increased interlayer spacing of Ti₃C₂T_x flakes. For a film prepared by a precursor solution with very high aniline content (1:500 sample), the (0002) peak shifted down to 4.7° corresponding to a c-lattice parameter (c-LP) of 37.8 Å.

Fig S2 shows the FTIR spectrum of the 1:500 sample. Compared to the samples prepared using low amounts of aniline, in this sample the corresponding peaks for PANI are intensified. This is due to the increased amount of PANI in final hybrid film which is in good agreement with the large interlayer spacing observed for this sample in the XRD experiments.

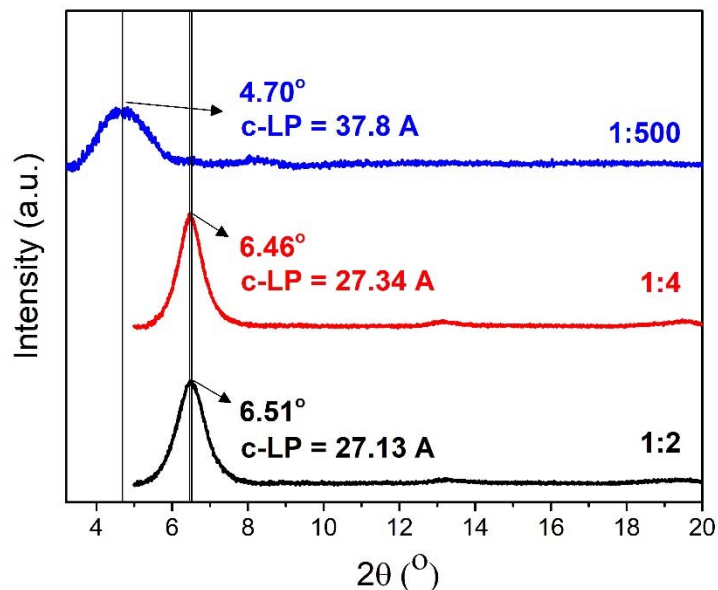


Figure S1. XRD patterns of the hybrid $\text{Ti}_3\text{C}_2\text{T}_x/\text{PANI}$ films prepared using different MXene to aniline ratios of 1:2, 1:4, and 1:500. By increasing the aniline to MXene ratio, the (0002) peak slowly shifts to lower angles and for very high ratio of 1:500 the intensity of MXene peaks decrease due to loss of ordering in the MXene/PANI films.

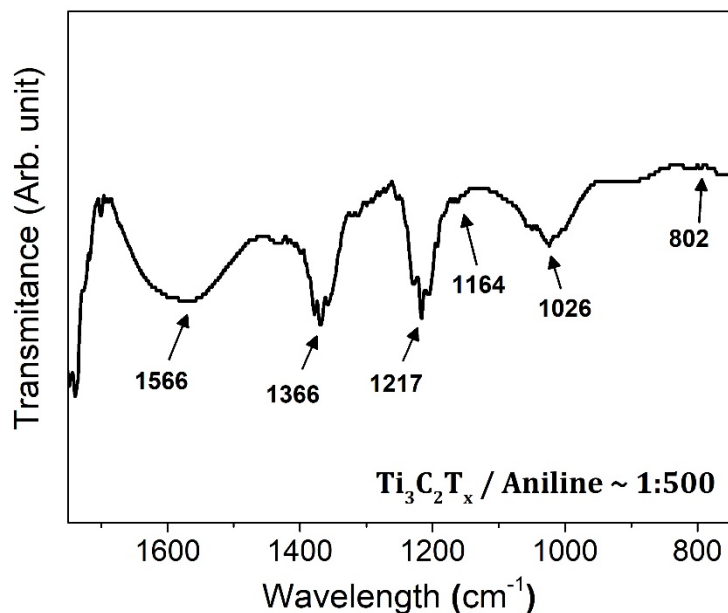


Figure S2. FTIR spectrum of $\text{Ti}_3\text{C}_2\text{T}_x/\text{PANI}$ hybrid films prepared using MXene to aniline ratio of 1:500. The peak at 1566 cm^{-1} corresponds to C=C stretching vibrations of quinonoid ring and the peaks at 1366 cm^{-1} and 1217 cm^{-1} correspond to C-N stretching vibrations. The peak at 1164 cm^{-1} can be assigned to C-H stretching of aromatic amine. Also, the transmittance peaks observed at 106 cm^{-1} and 802 cm^{-1} correspond to C-H out-of-plane vibration of the benzene ring.

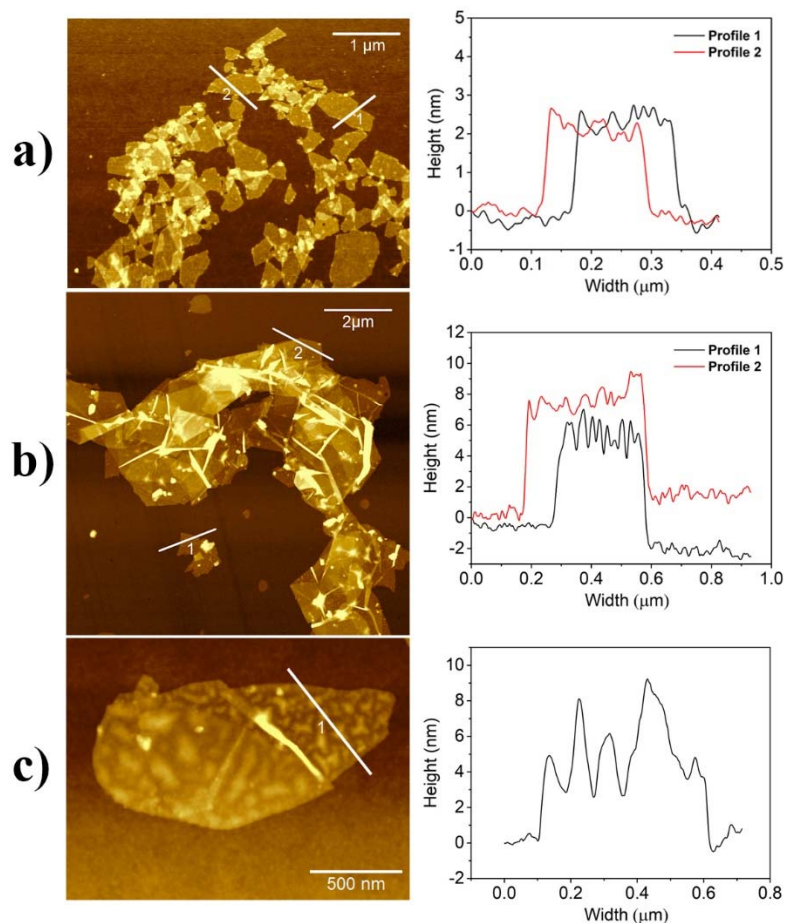


Figure S3. Atomic force microscopy (AFM) images and corresponding height profiles of (a) as synthesized $\text{Ti}_3\text{C}_2\text{T}_x$. (b) and (c) $\text{Ti}_3\text{C}_2\text{T}_x/\text{PANI}$ hybrids (with 1:2 MXene to aniline ratio) prepared in this study. The formation of island shape PANI chains on MXene flakes can be seen in these images. Thickness of single layer flakes of $\text{Ti}_3\text{C}_2\text{T}_x$ is ~ 2.7 nm. However, after polymerization of aniline on surface of MXene, the functionalized $\text{Ti}_3\text{C}_2\text{T}_x$ sheets are crumpled and their thicknesses increases to about ~ 6 nm.

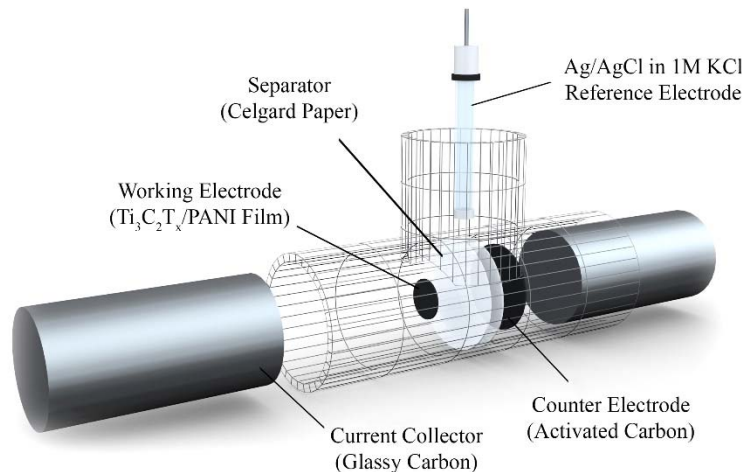


Figure S4. Schematic drawing of the three-electrode setup used in our study for electrochemical measurements. In our early experiments instead of glassy carbon current collectors we used stainless steel rods.

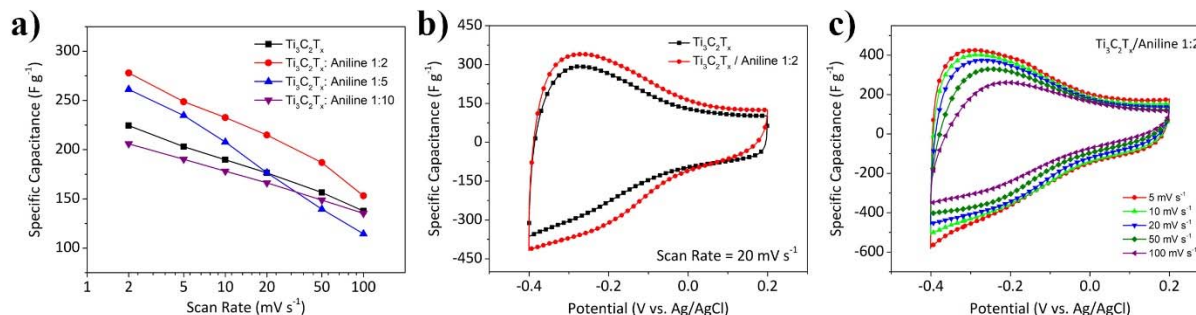


Figure S5. Electrochemical performance of hybrid electrode prepared using various MXene to aniline ratios. These experiments were done in our earlier electrochemical tests and using stainless steel rods as current collectors in a narrower potential window. (a) Capacitance of different hybrid films at different scan rates. A sample prepared using MXene to aniline ratio of 1:2 shows the highest specific capacitance at all scan rates. (b) CV curves of a $\text{Ti}_3\text{C}_2\text{T}_x$ electrode and $\text{Ti}_3\text{C}_2\text{T}_x$ /aniline (1:2) hybrid electrode. (c) CV curves of $\text{Ti}_3\text{C}_2\text{T}_x$ /PANI electrode at different scan rates of 5 mV s^{-1} to 100 mV s^{-1} in a potential window of -0.4V to +0.2 V (V vs Ag/AgCl) in $1\text{M H}_2\text{SO}_4$.

As it is shown in Figure S5a, by increasing the ratio of aniline monomer in the synthesis process beyond 1:2 (MXene to aniline), the electrochemical performance of the MXene/PANI hybrid electrodes decreases. As we have explained in the paper, the deposited PANI on MXene sheets does not directly contribute to the charge storage in the fabricated electrode as it is not

electrochemically active in the potential window that $Ti_3C_2T_x$ is active in sulfuric acid electrolytes. PANI only acts as a conductive spacer between the MXene layers. Therefore, the presence of excessive amounts of PANI in the hybrid electrodes' structure will increase the inactive component (deadweight) of the electrodes and reduces the specific capacitance of the hybrid material. This explains why the capacitance of the electrode with MXene to aniline ratios of 1:5 and 1:10 is lower than the electrodes with a ratio of 1:2.

Table S1. EDS results showing atomic percentage of different elements present in the pristine $Ti_3C_2T_x$ and $Ti_3C_2T_x$ /PANI hybrids for a sample prepared with high loading of aniline monomer.

	Ti	O	Cl	F	N
As prepared MXene	23.69%	24.59%	2.18%	10.22%	0%
After PANI deposition	9.88%	15.71%	0.89%	4.13%	33.3%

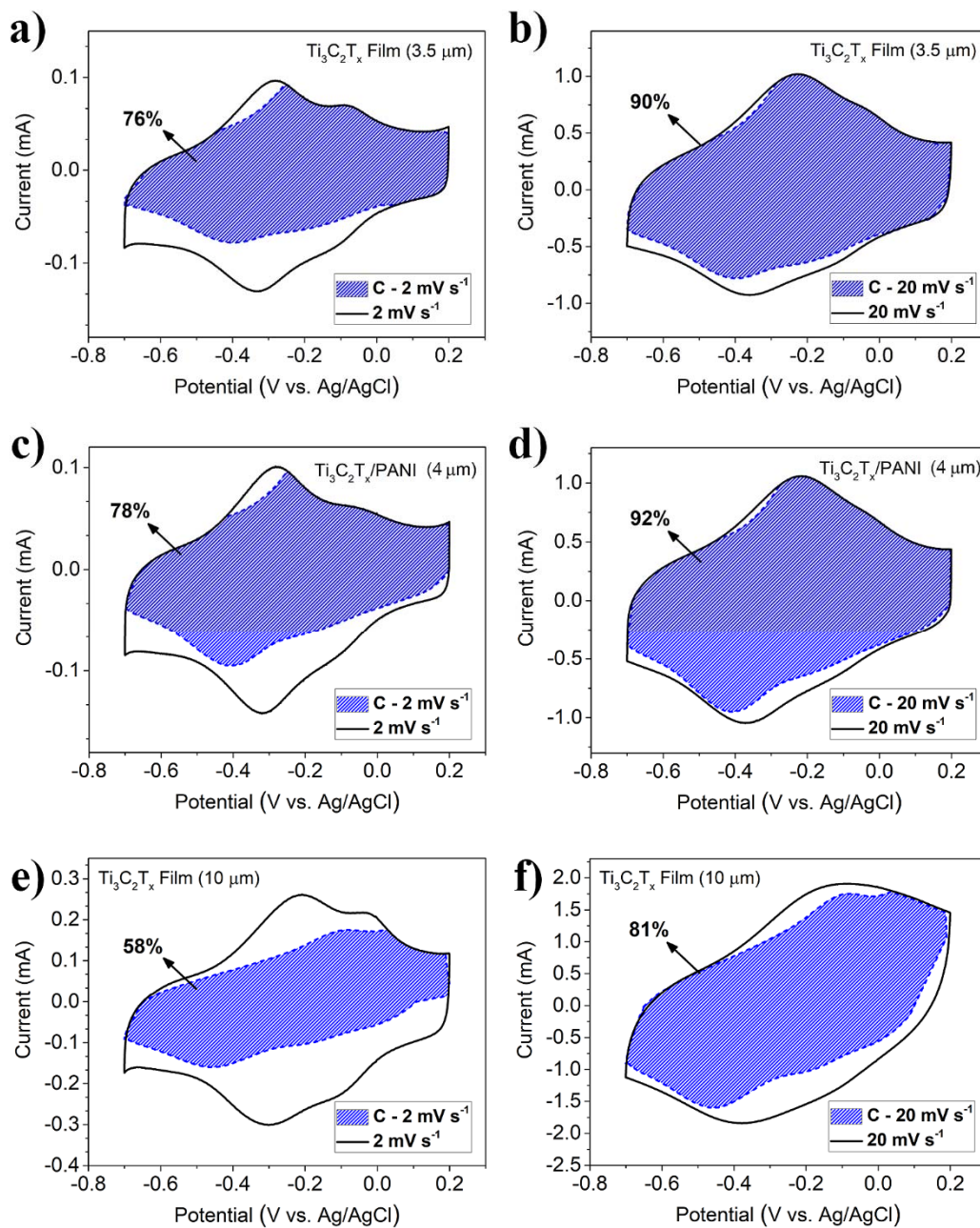


Figure S6. Capacitive charge storage contribution for a 3.5 μm thick $\text{Ti}_3\text{C}_2\text{T}_x$ electrode at scan rate of (a) 2 mV s^{-1} and (b) 20 mV s^{-1} , for a 4 μm thick $\text{Ti}_3\text{C}_2\text{T}_x/\text{PANI}$ hybrid electrode at scan rate of (c) 2 mV s^{-1} and (d) 20 mV s^{-1} , and for a 10 μm thick $\text{Ti}_3\text{C}_2\text{T}_x$ film at scan rate of (e) 2 mV s^{-1} and (f) 20 mV s^{-1} .

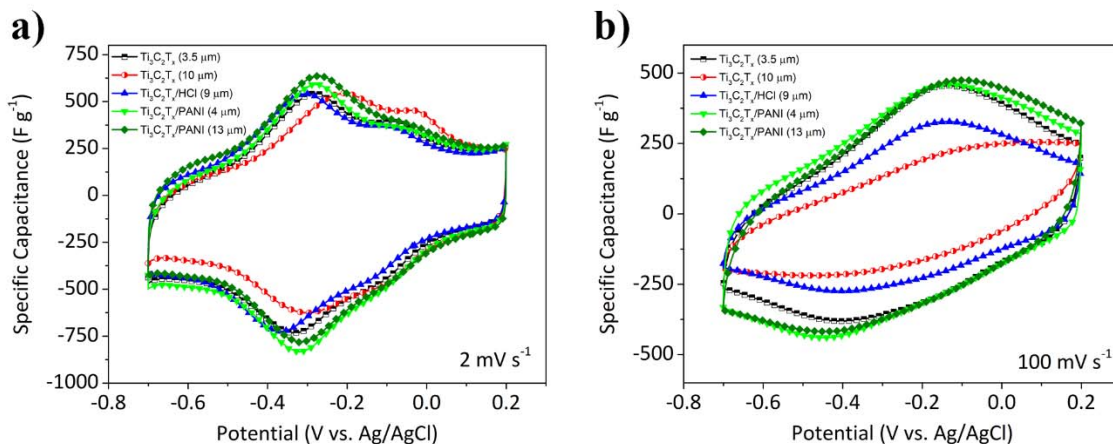


Figure S7. Comparison of CVs of MXene and MXene/PANI hybrid electrodes reported in this study at scan rates of (a) 2 mV s^{-1} and (b) 100 mV s^{-1} .

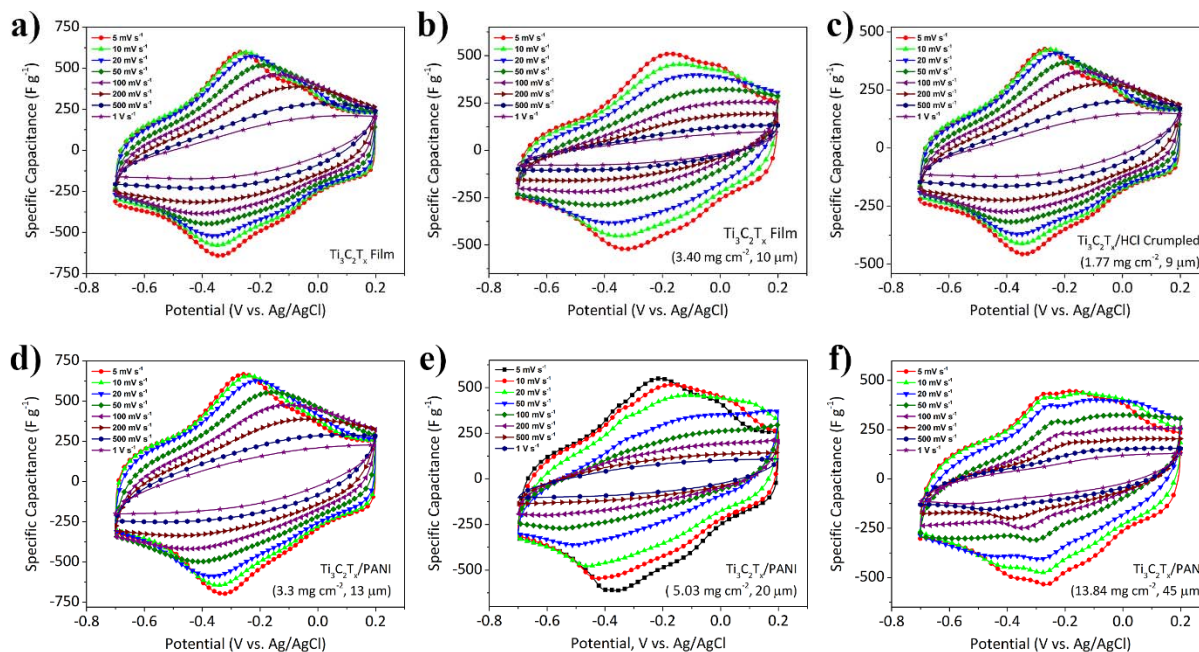


Figure S8. CV curves of (a) a $3.5 \mu\text{m}$ thick $\text{Ti}_3\text{C}_2\text{T}_x$ electrode, (b) a $10 \mu\text{m}$ thick $\text{Ti}_3\text{C}_2\text{T}_x$ electrode, (c) a $9 \mu\text{m}$ thick $\text{Ti}_3\text{C}_2\text{T}_x$ crumpled with HCl, (d) a $13 \mu\text{m}$ thick $\text{Ti}_3\text{C}_2\text{T}_x/\text{PANI}$ hybrid electrode, (e) a $20 \mu\text{m}$ thick $\text{Ti}_3\text{C}_2\text{T}_x/\text{PANI}$ hybrid electrode, and (f) a $45 \mu\text{m}$ thick $\text{Ti}_3\text{C}_2\text{T}_x/\text{PANI}$ electrode at scan rates ranging from 5 mV s^{-1} to 1 V s^{-1} .

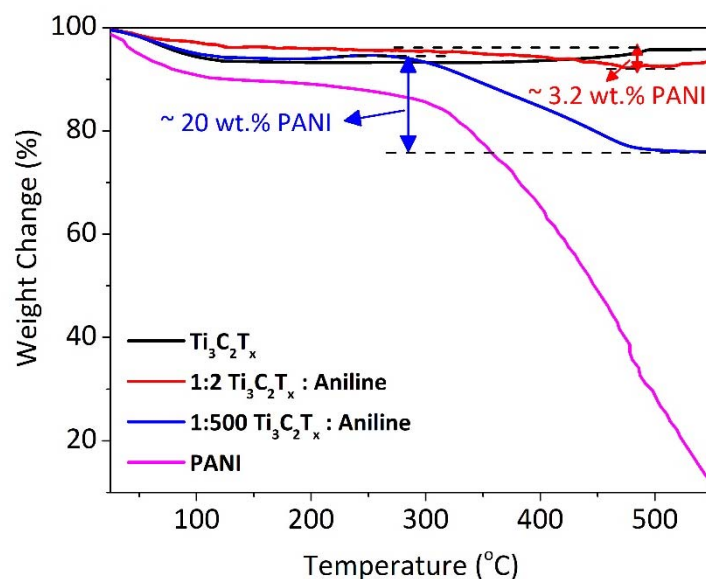


Figure S9. Thermogravimetric analysis (TGA) data of a pristine $\text{Ti}_3\text{C}_2\text{T}_x$ films, a hybrid film prepared using the $\text{Ti}_3\text{C}_2\text{T}_x$ to aniline ratio of 1:2, a hybrid film prepared using the $\text{Ti}_3\text{C}_2\text{T}_x$ to aniline ratio of 1:500, and pure PANI. The TGA experiments were carried out under O_2 atmosphere.

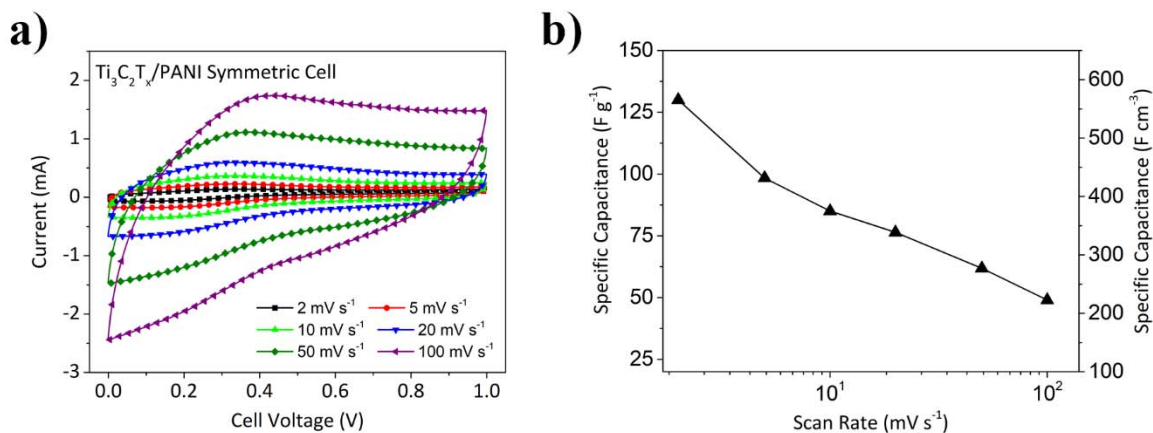


Figure S10. A symmetric supercapacitor prepared with two $\text{Ti}_3\text{C}_2\text{T}_x/\text{PANI}$ hybrid electrodes ($4 \mu\text{m}$ thickness) in $3\text{M H}_2\text{SO}_4$. (a) CVs at various scan rates ranging from 2 mV s^{-1} to 100 mV s^{-1} in a 1V voltage window and (b) Corresponding gravimetric and volumetric capacitances of the cell at different scan rates.

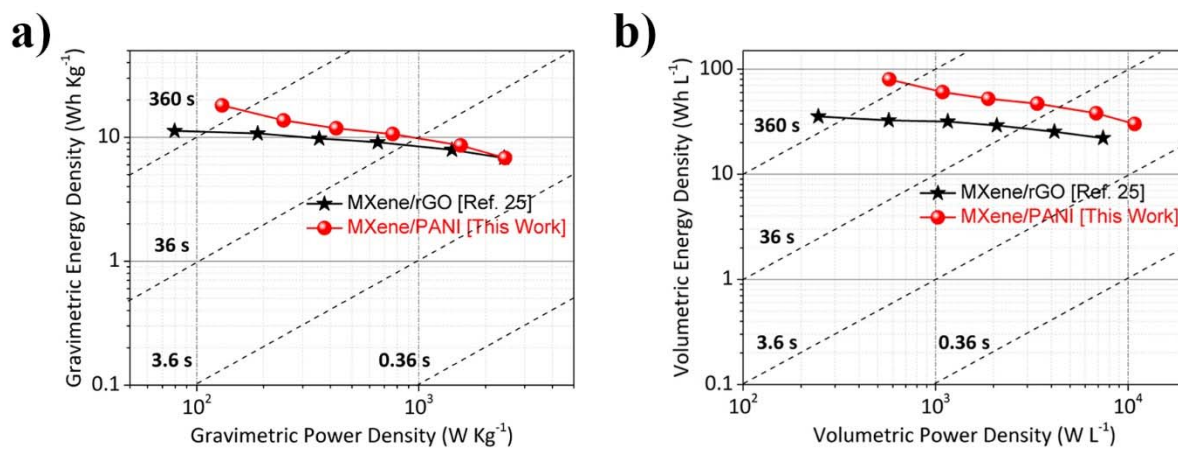


Figure S11. Ragone plots of the symmetric MXene/PANI supercapacitor with (a) gravimetric and (b) volumetric power and energy densities of the cell compared to a previously reported symmetric supercapacitor based on MXene/graphene hybrid electrodes.¹ (reference 1 in this document /reference 25 in the paper) The energy and power densities are calculated by considering the total mass of the active material in the symmetric cell.

References

- 1 J. Yan, C. E. Ren, K. Maleski, C. B. Hatter, B. Anasori, P. Urbankowski, A. Sarycheva and Y. Gogotsi, *Adv. Funct. Mater.*, 2017, **1701264**, 1701264.